

Hard-to-reach nuclei studied with deep-inelastic heavy-ion reactions

R. Broda^{1,a}, B. Fornal¹, W. Królas¹, T. Pawlat¹, J. Wrzesiński¹, D. Bazzacco², G. de Angelis³, S. Lunardi², and C. Rossi Alvarez²

¹ Niewodniczański Institute of Nuclear Physics, PL-31-342 Kraków, Poland

² Dipartimento di Fisica dell'Università and INFN Sezione di Padova, I-35131 Padova, Italy

³ INFN Laboratori Nazionali di Legnaro, I-35020 Legnaro (PD), Italy

Received: 15 January 2003 /

Published online: 23 March 2004 – © Società Italiana di Fisica / Springer-Verlag 2004

Abstract. Spectroscopic studies performed with deep-inelastic heavy-ion reactions are reviewed for two regions of neutron-rich nuclei. The identification of $\nu(h_{11/2})^n$ isomers in nearly complete series of Sn isotopes and the resulting systematic of $B(E2)$ values for isomeric transitions is presented and followed by the discussion of shell model states studied in neutron-rich Te isotopes including the new four neutron-hole isomers identified in ^{130}Te . Yrast spectroscopy studies of nuclei from the doubly magic ^{208}Pb region are described by outlining the highest spin states observed in the ^{208}Pb core nucleus. The $E3$ transitions observed abundantly in yrast decays are discussed within the framework of particle-octupole vibration coupling and the validity of a simple rule connecting energy shifts of octupole states built on one-particle states with the ones observed for two-particle states is demonstrated.

PACS. 21.60.Cs Shell model – 23.20.Lv γ transitions and level energies – 27.60.+j $90 \leq A \leq 149$ – 27.80.+w $190 \leq A \leq 219$

1 Introduction

For many years deep-inelastic heavy-ion reactions have been successfully used for spectroscopic studies of yrast excitations in nuclei that are not accessible in standard fusion evaporation processes employing stable nuclei as beams and targets. The proton and neutron flow taking place when the two heavy nuclei collide at energies significantly above the Coulomb barrier is governed by a strong tendency to equalize the N/Z ratios of the two final products. Consequently, by selecting the neutron-rich nuclei as beams and targets, one is able to produce many previously inaccessible isotopes located at the neutron-rich edge of the beta stability valley and far beyond it. Moreover, the new nuclei produced in such reactions are usually excited in a broad range of spin and energy, with preference for yrast state population. This feature allows to study high-spin state structures in nuclei which at present cannot be produced in standard fusion-evaporation processes —with emphasis on this particular difficulty one may qualify them as hard-to-reach nuclei. Experiments are made using thick targets located at the center of large gamma-detector arrays and selectivity is obtained exclusively by discrete gamma line analysis of the gamma coincidence data. In this way the observation is restricted to

gamma rays which are emitted from the recoiling products stopped in the target material, otherwise Doppler broadening prevents their detection. However, this condition is fulfilled for most of the yrast transitions as they usually involve state and/or feeding times longer than approximately 2 ps needed to stop the reaction product. Deep-inelastic heavy-ion reactions often produce hundreds of nuclei in the exit channel, each of them excited in a broad range of spin and excitation energy. Consequently, a very complex spectrum of gamma rays accompanying such reactions was hardly tractable until recently by any possible analysis. This situation has changed with the development of large multi-detector gamma arrays which offered excellent resolving power of the high-statistics multifold gamma coincidence data. First attempts to analyze such data started when the first, rather moderate in size, detector arrays became available for experiments [1, 2]; these were subsequently followed by the early spectroscopic applications [3–5]. During many years the GASP detector array played an important role in this research activity and the present conference which marks 10 years of its operation, gives us a chance to present few examples of spectroscopic results obtained with deep-inelastic heavy-ion reactions. Whereas the research program included many hard-to-reach nuclei scattered throughout all range of nuclide chart, ranging from the *spdf* shell light isotopes [6]

^a e-mail: broda@ifj.edu.pl

to the heavy actinides [7], we selected two examples which demonstrate systematic studies performed in two regions where the physics goals have been particularly well defined. Both of these studies were initiated at the very early stage of such experiments and have been continued until today, which gives the opportunity to present also the most recent results. The first example reviews the study of neutron-rich Sn and Te isotopes and includes recently obtained results on the high-spin states in ^{130}Te . The second one describes the high-spin state spectroscopy in nuclei around the doubly magic ^{208}Pb , with particular emphasis on the octupole core excitations which appear commonly in their yrast structures.

2 Isomeric states in neutron-rich Sn and Te isotopes involving $h_{11/2}$ neutrons

Systematic studies of yrast structures in the neutron-deficient $N = 82$ isotones above the ^{146}Gd identified a complete series of the 10^+ and $27/2^-$ isomeric states that arise from the maximum spin coupling of $(h_{11/2})^n$ protons correspondingly in even and odd isotones from ^{148}Dy [8] to ^{154}Hf [9]. The measured half-lives and isomeric $E2$ transition energies gave accurate $B(E2)$ values; their observed Z -dependence spectacularly demonstrated the validity of the shell model description and provided vital information on the filling of the $h_{11/2}$ proton orbital. The clarity of this results invoked interest to study an analogous phenomenon for the neutrons filling the $h_{11/2}$ orbital in the $Z = 50$ closed proton shell neutron-rich Sn isotopes extending through full range from $N = 66$ to $N = 80$. Few initial results were already available, since the corresponding 10^+ isomers have been extensively studied earlier in the ^{116}Sn and ^{118}Sn isotopes which can be easily produced in $(\alpha, 2n)$ reactions [10,11]. Also at the other end of the series, the 10^+ isomers in ^{128}Sn and ^{130}Sn have been identified earlier [12] in the beta decay of high-spin isomers of the corresponding In isotopes. Our attempts to search for similar isomers in other Sn isotopes started with the successful identification of the 10^+ isomer in the ^{120}Sn isotope produced using the ^7Li beam [13]. However, this case exhausted possibilities of using standard reactions to extend further such systematic and originally it was not clear in which way all the other neutron-rich Sn isotopes could be produced to ensure the population of the desired 10^+ and $27/2^-$ isomers. Here, the use of deep-inelastic heavy-ion reactions appeared to be an attractive idea, since early observations [1] indicated relatively intense population of high-spin states in the reaction products. The first experiment, using the pulsed ^{76}Ge beam of 325 MeV energy bombarding the ^{124}Sn target backed with lead, was performed at the Argonne NL with moderate array of 12 Ge gamma detectors and clearly established the 10^+ isomers in the ^{122}Sn and ^{124}Sn isotopes [3]. Crucial identifications of the expected $10^+ \rightarrow 8^+ \rightarrow 7^-$ two-gamma ray cascade isomeric decays were based on the observation of delayed coincidences with the known transitions occurring in the decays of the lower-lying 7^- isomers characterized by relatively long half-lives of 9.3 and 3.1 μs ,

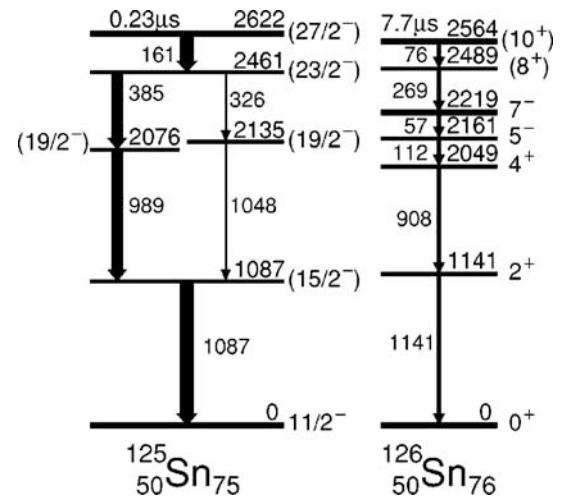


Fig. 1. Isomeric decay schemes for ^{125}Sn and ^{126}Sn .

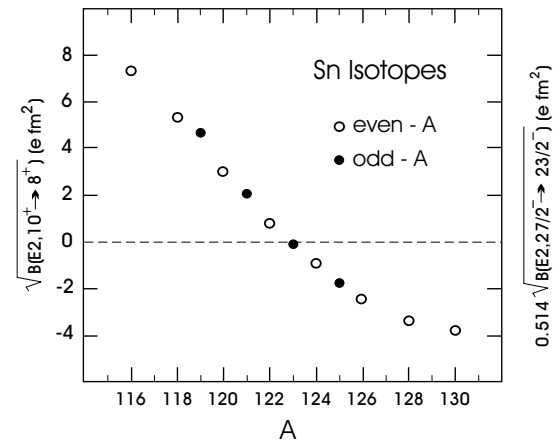


Fig. 2. $E2$ transition amplitudes for $(\nu h_{11/2})^n 10^+ \rightarrow 8^+$ and $27/2^- \rightarrow 23/2^-$ transitions in even- A and odd- A tin isotopes. As explained in [15], the $\sqrt{B(E2)}$ values for the odd- A nuclei are multiplied by 0.513 to compensate for different geometric factors entering the $v = 2$ and $v = 3B(E2)$ equations.

respectively. The measured 10^+ isomer half-lives of 62 μs in ^{122}Sn and 45 μs in ^{124}Sn as well as the corresponding $E2$ isomeric transition energies, gave two new points for the systematic of $B(E2)$ values. These encouraging results prompted a series of experiments in which a large variety of pulsed beams of ^{76}Ge , ^{80}Se , ^{136}Xe and ^{238}U was used to bombard the ^{124}Sn target and the data analysis was focused on a search for new isomers in other odd and even Sn isotopes. In odd $^{119,121,123}\text{Sn}$ isotopes the initial identification of the $(\nu h_{11/2} s_{1/2}) 19/2^+$ isomers [14] was a key step towards locating higher-lying $(h_{11/2})^n$ seniority $v = 3$ yrast states. The details concerning subsequent identifications of $27/2^-$ isomers in those odd Sn isotopes are described in refs. [15,16]. The most recent search was performed using the data from the ^{136}Xe and ^{238}U beam experiments and provided the identification of the $27/2^-$ isomer in ^{125}Sn and 10^+ isomer in ^{126}Sn [17]. The established decay schemes of those two isomers are shown in fig. 1 and the nearly complete systematic of experimental

$E2$ transition amplitudes for isomeric transitions in Sn isotopes is presented in fig. 2. The geometrical factor normalizing the $E2$ transition amplitudes for the seniority-3 and -2 isomers allowed to match both odd- A and even- A Sn isotope results and demonstrated their exceptionally smooth mass dependence. The systematic shown in fig. 2 summarizes many years of study of $(\nu h_{11/2})^n$ isomers by displaying the nearly complete $B(E2)$ -dependence on the $\nu h_{11/2}$ subshell occupation. It is obvious that the ^{123}Sn isotope with $N = 73$ is located very close to the point where the subshell is half-filled and the effective charge which determines the strength of the $E2$ transition induced by neutron particles and holes nearly cancel. Still missing are data points for ^{127}Sn and ^{129}Sn , where the expected $27/2^-$ isomers have yet to be found. Also the study of higher-seniority $(\nu h_{11/2})^n$ states in Sn isotopes remains an open and challenging question on the validity of shell model approach for more complex states.

Compared to tin isotopes, the presence of two additional protons in tellurium isotopes significantly alters the structure of yrast excitations. First of all, the new degree of freedom opened by the presence of two valence protons gives rise to the new set of states which are well known in the $N = 82$ ^{134}Te isotope studied with the fission gamma spectroscopy [18]. On the other hand, the coherent motion of these two protons with neutrons gives rise to the collectivity in the middle between the $N = 50$ and $N = 82$ major neutron shells; the ^{120}Te and ^{122}Te isotopes show profound vibrational structures. However, with increasing neutron number the collectivity is gradually giving way to structures involving shell model multiparticle configurations and isomers involving $h_{11/2}$ neutrons similar to Sn isotopes start to appear in heavier Te isotopes. This structural change was demonstrated in the spectroscopic investigation of neutron-rich Te isotopes performed with the use of $^{64}\text{Ni} + ^{130}\text{Te}$ deep-inelastic reactions [19]. Results of this study extensively discussed in [19] included even $^{126,128,130}\text{Te}$ isotopes in which 10^+ isomers were identified and odd $^{127,129,131}\text{Te}$ isotopes for which new yrast levels schemes were established. The most recent results which include the extended ^{130}Te level scheme shown in fig. 3, was obtained from the analysis of the $^{136}\text{Xe} + ^{232}\text{Th}$ experiment performed with the GAMMASPHERE array [7]. The new isomer established in this study was interpreted as the 15^- state arising from the maximum spin coupling of four neutron holes with configuration $(h_{11/2})^3 d_{3/2}$ and the lifetime value coinciding with the expected $E2$ transition rate. An important finding, that is indicated in the isomeric decay scheme of fig. 3, was the observation of gamma ray branches populating the lower-lying 10^+ isomer, which previously could not be located due to very low energy of the isomeric $E2$ transition [19]. The uniquely established energy of 19 keV for the unobserved $E2$ transition allowed to extract unique $B(E2)$ transition rate, which could then be added to the systematic of $10^+ \rightarrow 8^+$ $E2$ transitions in other Te isotopes. This systematic will be further discussed in the forthcoming publication [20] and compared with the Sn systematic indicating the difference due to the polarizing effect of two protons.

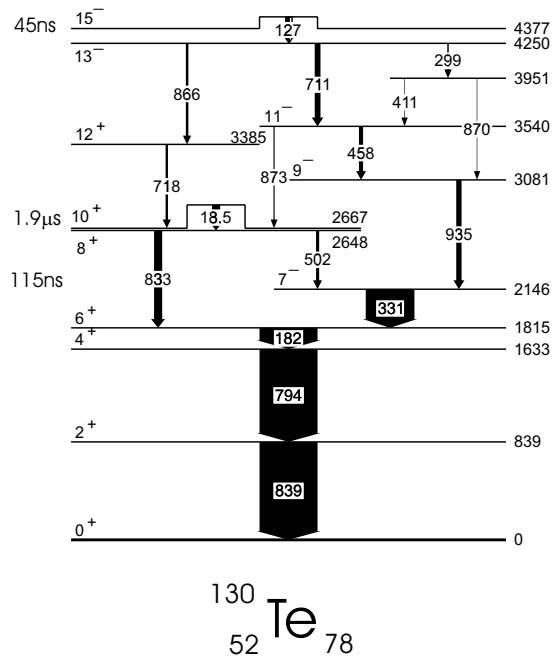


Fig. 3. Yrast scheme of ^{130}Te below the 15^- isomer.

3 Spectroscopy in the ^{208}Pb region and the role of octupole vibrations in yrast structures

Discrete gamma ray spectroscopy employing deep-inelastic heavy-ion reactions proved also to be an excellent technique to study high-spin states in hard-to-reach nuclei from the region of doubly magic ^{208}Pb . Already early experiments established previously unknown yrast structures in the ^{207}Pb above the $13/2^+$ isomer [4] and located many new high-spin states above the 10^+ isomer in the ^{208}Pb core nucleus [21]. The following experiments, in which the thick ^{208}Pb target was always bombarded by various heavy ion beams, identified high-spin states in ^{209}Pb [22], ^{210}Pb [23] isotopes and gave new results on more complex nuclei ^{211}Po [24], ^{211}Bi [25], as well as on probably the most attractive case studied recently of high-spin states in ^{206}Hg [26]. The combined sets of data from various experiments contain valuable complementary information on many other nuclei in the ^{208}Pb region and are the subject of continuous analysis. Parallel to the ongoing broad search for new yrast structures in other poorly studied isotopes, the analysis includes also efforts to extend information on nuclei that were already studied earlier. A typical example is here the doubly magic ^{208}Pb isotope for which subsequent experiments brought significant progress in establishing high-spin state structure up to very high spin and excitation energy range. Whereas important progress was reported in earlier publications [27], the most recent analysis of the $^{48}\text{Ca} + ^{208}\text{Pb}$ experiment revealed particularly rich information on the ^{208}Pb high-spin states reaching at least $I = 26$ spin values and 13.7 MeV excitation energy. The preliminary level scheme shown in fig. 4 and partly discussed in ref. [28] displays well the potential of the high-statistics data obtained with the GAMMASPHERE array, when the required events

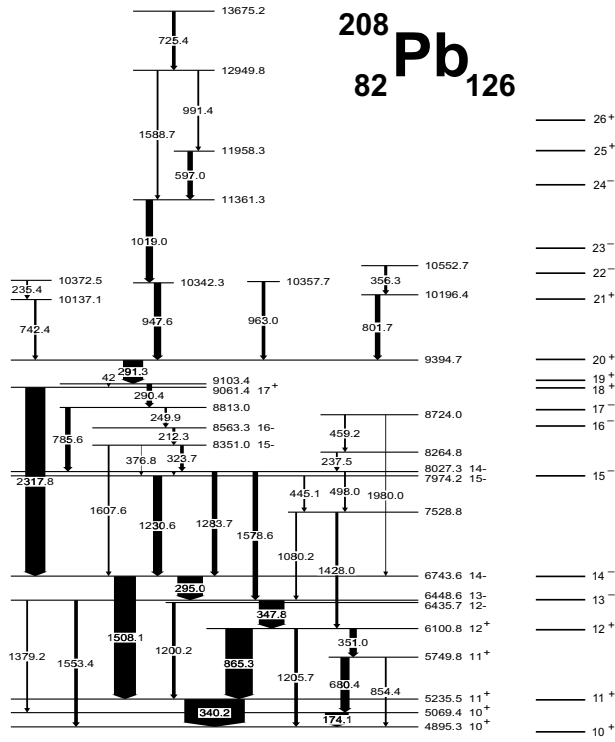


Fig. 4. High-spin states above the 10^+ isomer in ^{208}Pb . Yrast levels selected from shell model calculations are shown to the right.

can be selected in a very clean way. In this case the delayed coincidence gating making use of a very favorable lifetime of the 500 ns 10^+ isomer in ^{208}Pb served as a particularly suitable selection tool. At present, the difficulty in giving a satisfactory interpretation of the observed states comes from the lack of unambiguous spin-parity assignments and from the incomplete knowledge of effective interactions that enter shell model calculations for the complicated two-particle two-hole excitations. Nevertheless, calculations using the presently best available sets of interactions allow to select yrast levels which, with reasonable accuracy, indicate the range of spin values for the observed states, as shown in fig. 4. In the last part of this review we shall concentrate on octupole excitations which are abundantly observed in yrast structures of nuclei from the ^{208}Pb region. It has been already shown by the Canberra group [29] that the low-energy octupole vibration of the ^{208}Pb core contributes significantly to the low-lying states in the neighboring nuclei that have few valence particles. Extended discussion of several new examples, which demonstrated this phenomenon for high-spin states and were identified in our experiments, was presented in an earlier publication [30] and a thorough theoretical treatment of the particle-vibration coupling formalism was presented by Hamamoto [31]. Here we shall consider only the most general features that are evident when inspecting the high-spin state structures observed in the experiment. A very characteristic case is the situation in ^{209}Pb , where the lowest states involving pure single-particle neutron orbitals $g_{9/2}$ and $j_{15/2}$ are strongly affected by the coupling

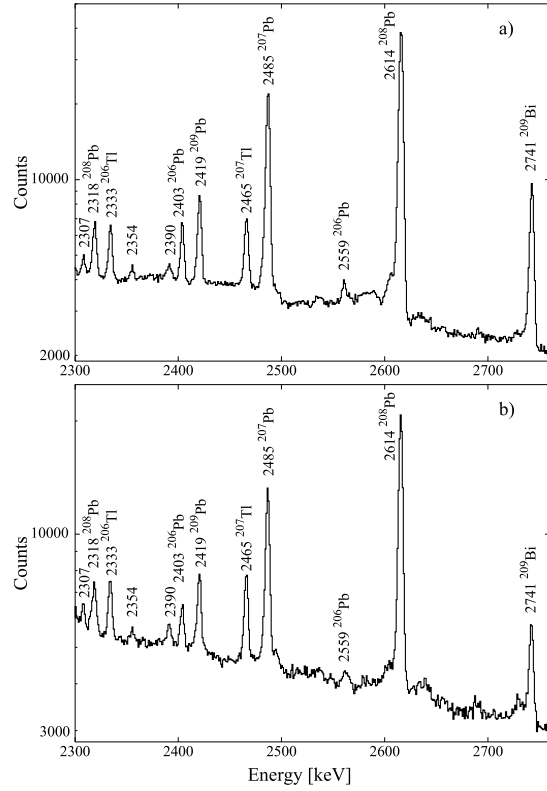


Fig. 5. The high-energy part of the total projection of the prompt-prompt E_γ - E_γ coincidence matrix from the experiment using a) the ^{208}Pb and b) the ^{136}Xe beam.

to the 3^- vibration of the ^{208}Pb core. The sizable energy shifts resulting in 1423 keV energy separation of the $9/2^+$ ground state and the lowest $15/2^-$ state are fully described by only one coupling matrix element and both states are connected by the fast (26 W.u.) $E3$ transition. In more complicated cases one often observes similarly fast $E3$ transitions of approximately 1.5 MeV energy within the yrast gamma decay of many neighboring nuclei. Such observations usually indicate involvement of the $j_{15/2}$ and $g_{9/2}$ neutron orbitals in the structure of correspondingly initial and final states, thereby serving as a clear guidance for their interpretation. Typical examples are the three $E3$ transitions observed in the ^{208}Pb level scheme of fig. 4. The apparently fast 1508 keV $E3$ transition connecting the 14^- state of $\nu j_{15/2} i_{13/2}^{-1}$ configuration with the 11^+ state of predominantly $g_{9/2} i_{13/2}$ character competes successfully with the slow $M1$ transition decay to the 13^- member state of the same $\nu j_{15/2} i_{13/2}^{-1}$ particle-hole excitation. Moreover, the two additional $E3$ branches of 1379 and 1553 keV are observed in the decay of this 13^- state to the two lowest 10^+ states. The measured $E3$ branching in this case provides important information on $\nu g_{9/2} i_{13/2}^{-1}$ amplitudes which contribute to the structure of both 10^+ states.

However, the most interesting observed feature is the stretched coupling of the 2615 keV 3^- octupole vibration of the ^{208}Pb core with very pure and simple two-particle states. Usually, states of maximum spin coupling involving

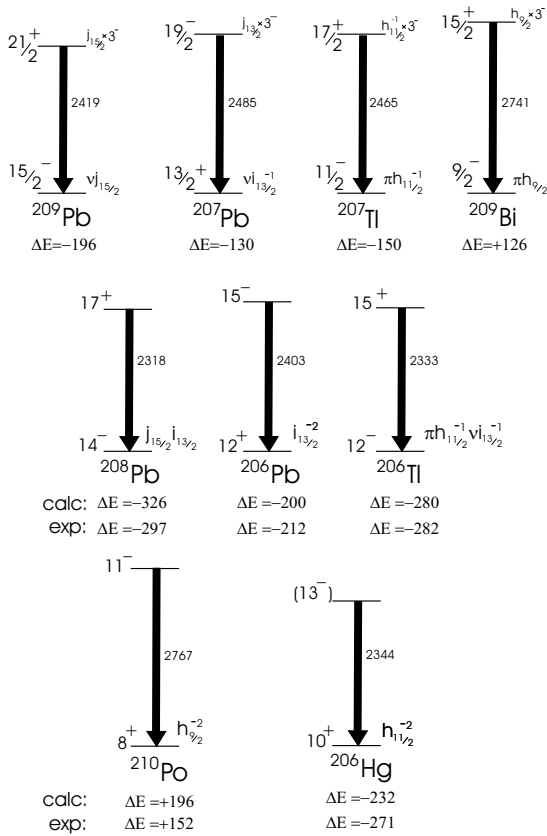


Fig. 6. Yrast $E3$ transitions observed above high-spin states in nuclei from the ^{208}Pb region.

such simple structures assume the most prominent yrast position and often become isomeric states. The lowest 3^- core excitation is then energetically the cheapest way to acquire higher spins; consequently, the stretched coupling of this octupole vibration with simple two-particle (hole) states produces states that are strongly populated in the yrast decay. Figure 5 displays the high-energy part around 2.6 MeV of total gamma prompt coincidence projections obtained in two experiments using the ^{208}Pb and ^{136}Xe beams. Practically, all gamma lines seen in those spectra could be identified as transitions de-exciting states which arise from stretched coupling of the octupole vibration with very simple shell model high-spin states known in various nuclei of the ^{208}Pb region. The fairly rich collection of such transitions allows to compare systematically the experimental energy shifts of the octupole vibration built on two particle (hole) states with shifts observed for octupole coupling to individual particles (holes). It turns out that simple addition of individual shifts for stretched coupling and more general calculation by simple angular momentum recoupling reproduces surprisingly well shifts observed for complex states. The validity of such simple approach is illustrated in fig. 6, where the collection of observed octupole excitations is displayed for a number of nuclei located in the closest neighborhood of ^{208}Pb . The upper part of fig. 6 displays basic cases of $E3$ excitations coupled to high- j one-particle (hole) states that are constituents of two-particle (hole) states. The corresponding

energy shifts with respect to the 2615 keV core excitation are marked below. It is worthwhile to note that apart from the ^{209}Bi case, all other $E3$ transitions were identified for the first time in experiments using deep-inelastic heavy-ion reactions. In the lower part of fig. 6, the $E3$ transitions observed above the two-particle (hole) states are shown. The indicated configurations of basic states define individual constituents from the upper part which naturally were used to calculate energy shifts by simple addition or angular momentum recoupling. The comparison of the observed and calculated energy shifts displayed below each $E3$ transition indicates very good agreement of both values for nearly all cases. Although the interaction is weak enough to ensure the main importance of linear terms, the quality of the observed agreement is rather surprising and invites further experimental search for other suitable cases. The new, particularly attractive case observed recently in the high-spin state study of ^{205}Tl is presented by J. Wrzesiński (p. 57).

In conclusion, the systematic spectroscopic study of hard-to-reach nuclei from two regions of the nuclide chart were reviewed to demonstrate the power of the gamma coincidence experiments using deep-inelastic heavy-ion reactions. The extensive study of isomeric states involving $h_{11/2}$ neutrons in neutron-rich Sn and Te isotopes displayed rather transparent interpretation within simple shell model approach and provided information on the varying occupation of the $h_{11/2}$ orbital as well as indicated strong polarizing effects of two protons present in Te isotopes. The results concerning the high-spin state structure of nuclei from the ^{208}Pb region were reviewed with particular emphasis on states involving the coupling of simple shell model states with octupole vibrations of the ^{208}Pb core.

The results described in the present review and published earlier were obtained in collaboration with several research groups besides those using principally the GASP array and included in the authors list. The quoted references include also all the other names. The authors express their warm gratitude particularly to P.J. Daly, W.Z. Grabowski, C.T. Zhang, J. Blomqvist, K.-H. Maier, M. Rejmund, J. Cocks, P. Butler, R.V.F. Janssens and M. Carpenter for active participation and often expert guidance in this research. This work was supported by the Polish Scientific Committee under Grant No. 2P03B-074-18.

References

1. R. Broda *et al.*, Phys. Lett. B **251**, 245 (1990).
2. R. Broda *et al.*, Phys. Rev. C **49**, R575 (1994).
3. R. Broda *et al.*, Phys. Rev. Lett. **68**, 1671 (1992).
4. M. Schramm *et al.*, Z. Phys. A **344**, 121 (1992).
5. T. Pawlat *et al.*, Nucl. Phys. A **574**, 623 (1994).
6. B. Fornal *et al.*, Phys. Rev. C **49**, 2413 (1994).
7. J.F.C. Cocks *et al.*, Phys. Rev. Lett. **78**, 2920 (1997).
8. P.J. Daly *et al.*, Z. Phys. A **298**, 173 (1980).
9. J.H. McNeill *et al.*, Phys. Rev. Lett. **63**, 860 (1989).
10. M. Ishihara *et al.*, in *Proceedings of the International Conference on Nuclear Physics, Munich, August 27-September 1, 1973*, edited by J. de Boer, H.J. Mang, Vol. **1** (North-Holland, Amsterdam, 1973) p. 256.

11. A. Van Poelgeest *et al.*, Nucl. Phys. A **346**, 70 (1980).
12. B. Fogelberg *et al.*, Nucl. Phys. A **352**, 157 (1981).
13. S. Lunardi *et al.*, Z. Phys. A **328**, 487 (1987).
14. R.H. Mayer *et al.*, Z. Phys. A **342**, 247 (1992).
15. R.H. Mayer *et al.*, Phys. Lett. B **336**, 308 (1994).
16. P.J. Daly *et al.*, Phys. Scr. T **56**, 94 (1995).
17. C.T. Zhang *et al.*, Phys. Rev. C **62**, 57305 (2000).
18. C.T. Zhang *et al.*, Phys. Rev. Lett. **77**, 3743 (1996).
19. C.T. Zhang *et al.*, Nucl. Phys. A **628**, 386 (1998).
20. R. Broda *et al.*, to be published in Phys. Rev. C.
21. M. Schramm *et al.*, Z. Phys. A **344**, 363 (1993).
22. M. Rejmund *et al.*, Eur. Phys. J. A **1**, 261 (1998).
23. M. Rejmund *et al.*, Z. Phys. A **359**, 243 (1997).
24. B. Fornal *et al.*, Eur. Phys. J. A **1**, 355 (1998).
25. G.J. Lane *et al.*, Nucl. Phys. A **682**, 71c (2001).
26. B. Fornal *et al.*, Phys. Rev. Lett. **87**, 212501 (2001).
27. J. Wrzesiński *et al.*, Eur. Phys. J. A **10**, 259 (2001).
28. R. Broda *et al.*, *Proceedings of the 7th International Spring Seminar on Nuclear Physics, Maiori 2001*, edited by A. Covello (World Scientific, Singapore, 2002).
29. A.P. Byrne *et al.*, Phys. Rev. Lett. **80**, 2077 (1998) and references therein.
30. M. Rejmund *et al.*, Eur. Phys. J. A **8**, 161 (2000).
31. I. Hamamoto, Phys. Rep. **10**, 63 (1974).